Magnetic Properties of Fe Microstructures with Focused Ion Beam-Fabricated Nano-Constrictions

Igor V. Roshchin, Jun Yu, Andrew D. Kent, Gary W. Stupian, and Martin S. Leung

***Abstract*—Studies of the magnetic properties of Fe microfabricated wires with a mechanically stable 40 to 120 nm-wide constriction produced with focused ion beam are reported. The 2 to 20 μm-wide wires are fabricated by photolithography from 3 nm and 25 nm-thick epitaxial (110) bcc Fe films. This fabrication method appears to preserve the magnetic properties of the constriction. The structures are studied by MFM and by magneto-optic Kerr effect (MOKE) measurements. The ratio of the wire linewidth to its thickness determines the demagnetization factor and, therefore, influences the coercivity of the wire. Both a step in the width of the wire and a nano-constriction in the middle of the wire are found to be domain wall (DW) pinning centers.**

***Index Terms*—Fe, ferromagnetic microstructures, FIB, iron epitaxial thin films, Kerr effect, magnetization reversal, MFM, nano-structures.**

I. Introduction

SUB-MICRON scale ferromagnetic wires are a topic of great interest. Different aspects of studies related to this type of structures include: magnetic properties of geometrically confined structures [1], ballistic transport, and quantum size effects, when the wire has only a few quantum conduction channels [2], [8]. Planar nano-scale constrictions in ferromagnetic wires have been fabricated by a few different methods including straining a thin microfabricated wire (break junction) [3], and e-beam and photolithography. While the first approach allows one to study very narrow wires, it does not usually result in mechanically stable structures. Both e-beam and photolithography have minimum size limits. Although with e-beam lithography it is possible to produce ∼10 nm features in resist, the transfer of these features into a thin ferromagnetic material is not yet a well established process.

In this paper we report the successful fabrication of nano-scale constrictions in photolithographically defined micron-scale wires by making a cut with a focused ion beam (FIB), and an investigation of their magnetic properties using magneto-optical Kerr effect (MOKE) measurements and magnetic force microscopy (MFM).

Manuscript received October 13, 2000.

I. V. Roshchin, J. Yu, and A. D. Kent were supported by DARPA-ONR, Grant N00014-96-1-1207. G. W. Stupian and M. S. Leung were supported by the United States Air Force under Contract F04701-00-C-0009.

I. V. Roshchin and A. D. Kent are with the Department of Physics, New York University, New York, NY 10003 USA (e-mail: {ivr1; andy.kent}@nyu.edu).

J. Yu was with the Department of Physics, New York University. He is now with Advanced Materials Research Institute, University of New Orleans, Seagate Research, Pittsburgh, PA 15203 USA.

G. W. Stupian and M. S. Leung are with the Electronics and Photonics Laboratory, Laboratory Operations, The Aerospace Corporation, El Segundo, CA 90245.

Publisher Item Identifier S 0018-9464(01)07259-4.

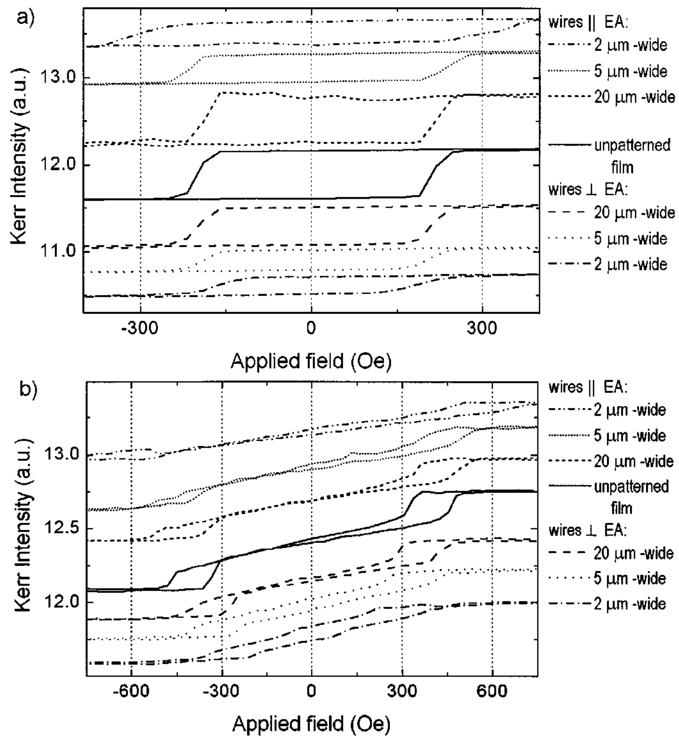

Fig. 1. MOKE measurements: Magnetization of 25 nm-thick unpatterned epitaxial Fe film and wires oriented parallel and perpendicular to the easy magnetic axis when (a) the magnetic field is applied along the easy axis; (b) the magnetic field is applied perpendicularly to the easy axis.

II. Sample Preparation and Characterization

Iron films are epitaxially grown on a-axis $(11\bar{2}0)$ sapphire substrates by UHV e-beam evaporation. First, a 3–5 nm-thick Mo seed layer is deposited at ∼610 °C at a rate of 0.02–0.08 nm/s. Then 3 nm or 25 nm of iron are deposited at ∼ 240 °C at a similar rate. To protect against corrosion, the film is capped with a 2.5 nm of Al, thermally evaporated at a rate of 0.02–0.05 nm/s. Earlier X-ray analysis of similar films demonstrated (110) Fe-film orientation, and that the Fe in-plane $[1\bar{1}1]$ axis is parallel to [0001] direction of the sapphire substrates [4]. An anisotropic in-plane strain in these films induces an in-plane uniaxial magnetic anisotropy with the easy axis (EA) along the [001] direction in addition to the cubic anisotropy, characteristic of bulk bcc Fe [5]. The hysteresis loop of an unpatterned (110) Fe film with the magnetic field applied parallel to the $[1\bar{1}0]$ direction is consistent with two and four-fold in-plane components of the magnetic anisotropy [see Fig. 1(b)]) [4].

From these Fe films, two types of structures are fabricated using a standard photolithography process with subsequent

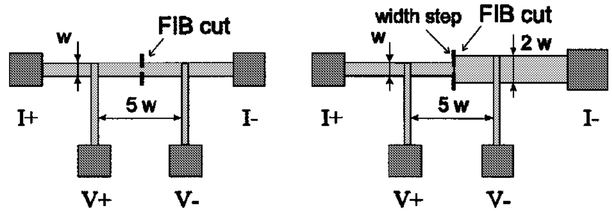

Fig. 2. Sketch of two types of single wires with a FIB-fabricated constriction.

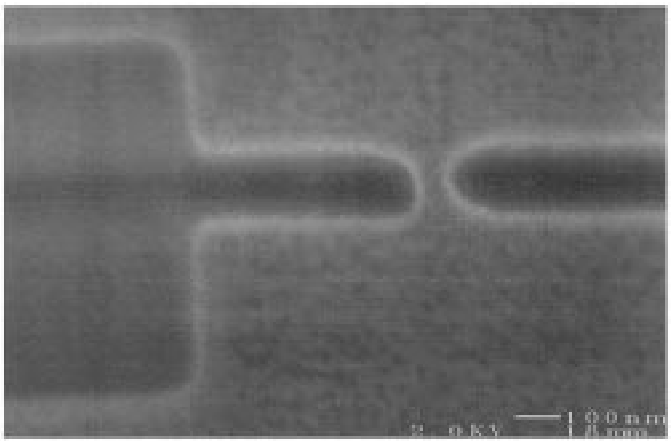

Fig. 3. SEM image of a typical sub-100 nm cut [same as in Fig. 4(b), rotated by 90°] fabricated with FIB in a 25 nm-thick Fe wire. The scale bar is 100 nm.

Ar-ion milling: single wires for transport measurements and arrays of wires for MOKE measurements. Both uniform width wires and wires with a 1 : 2 step in the wire width are fabricated in three base wire linewidths (w): 2 μm, 5 μm, and 20μm. All wires are fabricated in two orientations: parallel and perpendicular to the [001] EA of Fe. The wires in the array are spaced by $5w$.

The magnetic properties and the magnetization reversal process of *arrays* of wires are studied via longitudinal MOKE hysteresis loops, using ~200 μm-wide laser beam. Individual wires are studied with a Digital Instruments (DI) Dimensions-3000 MFM with an *in-situ* electromagnet. 50 nm-thick Co alloy coated silicon MESP DI probes (~400 Oe coercivity, 10^{-13}\emu moment) are used for imaging.

A nano-constriction in the middle of single wires is fabricated by making two cuts toward each other from opposite sides of the wire (see Fig. 2). The cuts are made with a FIB, FEI-610, using 25 kV gallium ions (7–8 pA beam current). To avoid limitations imposed by the small field of view at high magnification, wide (~730 nm) "notch cuts" are performed first in order to narrow down the area to be cut. Then, one of two types of ~1 μm-long cuts are performed: a "line cut," when the width of the cut is determined by the ion-beam width (of the order of 100 nm), or a wider (~300 nm) "box cut." The width of the constriction is varied from 40 nm to 120 nm as confirmed by both SEM (Fig. 3) and AFM images [Fig. 4(a)].

Observation of the magnetic poles between the notch cuts, and curving of the poles inside the constriction neck (not shown here), shows that the constrictions are magnetic, at least at some large (~100 nm) scale.

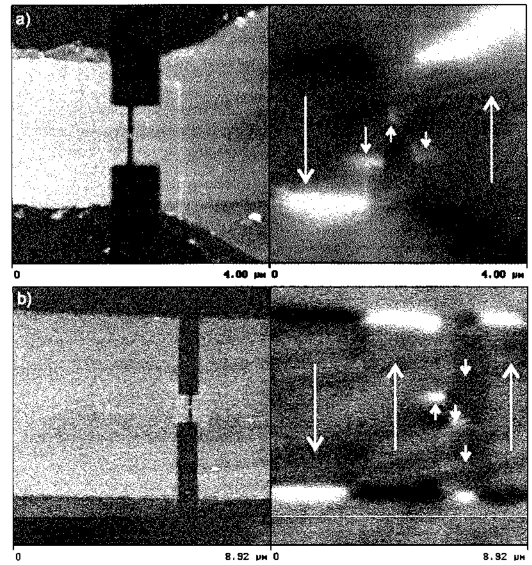

Fig. 4. AFM (left) and zero-field MFM (right) images of typical sub-100 nm cuts fabricated with FIB in a 25 nm-thick, nominally 5 μm (a) and 2–4 μm-wide (b) Fe wires with a domain wall trapped (a) in the middle of the cut, (b) at the left side of the cut.

TABLE I
SUMMARY OF MAGNETIC PARAMETERS

Field along	Field value (Oe)	Unpatterned film	2 μm -wide wires perpendicular to the easy axis	2 μm -wide wires parallel to the easy axis
Hard axis	H_N	379	203	527
	H_S	525	466	757
Easy axis	H_N	173	145	218
	H_S	262	291	379

III. RESULTS AND DISCUSSION

When a wire is patterned in a uniaxial ferromagnetic film, the orientation and the size (width-to-thickness ratio) of the wire determine the relation between the magnetocrystalline energy and the wire magnetostatic energy (due to the demagnetization factor). The hysteresis loops of 25 nm-thick wires of three different linewidths (2 μm, 5 μm, and 20 μm) and two orientations: parallel and perpendicular to the EA for both longitudinal and transverse fields, are presented in Fig. 1. Table I summarizes some of the magnetic field values obtained from these plots.

As the width of the wires parallel to the EA increases or the width of the wires perpendicular to the EA decreases (from the top curves plotted to the bottom ones), all characteristic fields, nucleation field, saturation field and coercivity field ($H_{\rm N}$, $H_{\rm S}$, and $H_{\rm c}$) decrease. When the wires are parallel to the EA, the effective anisotropy $K_{\rm eff}$ is a sum of the magnetocrystalline and the shape anisotropy. When the wires are perpendicular to the EA, there is a competition between these two energies.

There are two factors that contribute to the observed trend: First, the demagnetization factor in this 2 μm-wide, 25 nm-thick wire starts playing a role. The effect of the wire width is much smaller or is not observed in the same type of wires, when the thickness is 3 nm. Second, as the wire width is reduced, the domain size is also reduced. The smaller size of the domains can make the nucleation of the reversal process easier.

These MOKE measurements results are consistent with the results obtained by MFM imaging of the reversal process in these wires. There is a general correlation between the values of the H_N and H_S obtained from the MOKE and the values of the applied magnetic field corresponding to the appearance of the first domain with the reversed magnetization, and to the reversal of the magnetization in the whole wire, respectively. However, there is a difference in values obtained by MOKE and by MFM imaging. This is attributed to an additional local magnetic field due to the stray field of the MFM probe. It is worth noting that when the applied field is much smaller than the H_N or when it is zero, the MFM images are stable in time and the magnetic configuration of the sample is not affected by the MFM probe. Good resolution of the MFM images is confirmed by the possibility to resolve at a higher magnification the Neél cross-tie domain walls (DW's) that are present in Fig. 4(a).

A. Magnetic Easy Axis Perpendicular to the Wires

When the wires are perpendicular to the EA, Neél cross-tie DW's are observed in the absence of the applied magnetic field and in small fields applied perpendicular to the wire.

The MFM measurements show that the $1:2$ step in the width of the 2 μm-wide wires is a pinning center for DW's, although not a very strong one. This effect is not observed in wider wires (5 μm–10 μm and 20 μm–40 μm). There are two possible reasons for this. First, the difference in the effective coercivity of the two sides of the wires is very small when the width is much larger than the thickness of the wires due to very small difference in the demagnetization factor in this case. Second, in wider wires, especially in 20 μm-wide wires, the density of the cross-wire domains in the wider wires is smaller, and Lifshitz-type domains [7] which have smaller DW surface are more energetically favorable. We do not observe DW's of Lifshitz domains trapped at the width step.

The wires are again imaged with the MFM after the 40–120 nm constrictions are fabricated with FIB. Several effects related to these constrictions are observed. First, the constriction is a strong pinning center for the DW in the wire, for both, longitudinal and transverse field configurations. Second, the saturation field increases by approximately 40 Oe when the field is applied along the EA, as determined by MFM.

When a DW is trapped at the constriction or in a close proximity to it, the magnetic configuration inside the constriction is drastically modified. When the DW is trapped at the neck of the constriction, a domain configuration with the central symmetry with respect to the middle of the constriction is formed, where the domains on the two sides of the constriction have an opposite magnetization [Fig. 4(a)]. When the DW is at the side of the constriction, i.e., in the wider constriction region, a clover-like configuration is formed just in one half of the constriction as shown in Fig. 4(b). In some cases a more complicated configuration with larger number of "leaves" (8 or 12) is formed. These configurations minimize the magnetostatic energy locally inside the constriction. Micromagnetic simulations will be used to study this behavior in more detail.

B. Magnetic Easy Axis Parallel to the Wires

When the wires are parallel to the magnetocrystalline EA, and the field is parallel to the wire and to the EA, a head-to-head DW is expected. However, this type of wall costs a lot of magnetostatic energy. We observe a meandering staircase-like wall, similar to what has been seen in thin magnetic films with low anisotropy [6]. We are able to trap a DW at the step width in a narrow range of the magnetic field, when it is applied perpendicularly to the EA. No DW trapping at the constriction is observed in either longitudinal or transverse field configuration.

IV. Summary

We observe that the width and the orientation of thin (3 nm and 25 nm) wires determines their nucleation, saturation and coercivity fields. The possibility of trapping DW's at the step in the wire width for 2 μm-wide wires is demonstrated. Using FIB, we produce mechanically stable sub-100 nm constrictions in these wires, which seem to preserve their magnetic properties. When the wire is perpendicular to the magnetic EA, the constriction is a strong DW pinning center, which leads to an increase in the saturation field H_S. These structures thus enable new experimental studies of geometrically confined DW's.

Acknowledgment

The authors would like to thank S. S. P. Parkin for fruitful discussions. Microfabrication is done at the CNF, Project 588-96.

References

[1] P. Bruno, *Phys. Rev. Lett.*, vol. 85, p. 3165, 2000.
[2] G. Tatara, Y.-W. Zhao, M. Muñoz, and N. Garcia, *Phys. Rev.*, vol. 83, p. 2030, 1999.
[3] C. J. Muller, J. M. van Ruitenbeek, and L. J. de Jongh, *Physica C*, vol. 191, p. 485, 1992.
[4] J. Yu, U. Rüdiger, A. D. Kent, L. Thomas, and S. S. P. Parkin, *Phys. Rev. B*, vol. 60, p. 7351, 1999.
[5] B. M. Clemens, R. Osgood, A. P. Payne, B. M. Lairson, S. Brennan, R. L. White, and W. D. Nix, *J. Magn. Magn. Mater.*, vol. 121, p. 37, 1993.
[6] A. Hubert and R. Schäfer, *Magnetic Domains: The Analysis of Magnetic Microstructures*. Berlin-Heidelberg: Springler-Verlag, 1998, pp. 451–452.
[7] L. D. Landau, E. M. Lifshitz, and L. P. Pitaevskii, *Electrodynamics of Continuous Media*, 2nd ed. Oxford, England: Butterworth-Heinenann, 1984.
[8] N. Garcia, *Appl. Phys. Lett.*, vol. 77, p. 1351, 2000.